J. Fluid Mech. (1972), *vol.* 52, *part* 1, *pp.* 179–191
Printed in Great Britain

On the interaction of surface and internal waves

By A. E. GARGETT†
Institute of Oceanography, University of British Columbia, Vancouver, B.C.
AND B. A. HUGHES
Defence Research Establishment Pacific, F.M.O., Victoria, B.C.

(Received 8 May 1971 and in revised form 18 October 1971)

The steady-state interaction between surface waves and long internal waves is investigated theoretically using the radiation stress concepts derived by Longuet-Higgins & Stewart (1964) (or Phillips 1966). It is shown that, over internal wave crests, those surface waves for which $c_{g0}\cos\phi_0 > c_i$ experience a change in direction of propagation towards the line of propagation of the internal waves and their amplitudes are increased. Here c_{g0} is the surface-wave group speed at $U = 0$, ϕ_0 is the angle between the propagation direction of the surface waves at $U = 0$ and the propagation direction of the internal waves, and c_i is the phase speed of the internal waves. If $c_{g0}\cos\phi_0 < c_i$ the direction of the surface waves is turned away and their amplitudes are decreased. Over troughs the opposite effects occur.

At positions where the local velocity of surface-wave energy transmission measured relative to the internal wave phase velocity is zero, i.e. $\mathbf{c}_g + \mathbf{U} - \mathbf{c}_i = 0$, there is a singularity in the energy of the surface waves with resulting infinite amplitudes. It is shown that at these critical positions two wavenumbers which were real and distinct on one side coalesce and become complex on the other. The critical positions are thus shown to be barriers to the propagation of those wavenumbers. It is also shown that there is a critical position representing the coalescence of three wavenumbers. Surface-wave crest configurations are shown for three numerical examples. The frequency and direction of propagation of surface waves that exhibit critical positions somewhere in an internal wave field are shown as a function of the maximum horizontal surface current. This is compared with measurements of wind waves that have been reported elsewhere.

1. Introduction

The association of internal waves and the regular banded patterns of either surface slicks or surface roughnesses, often observed in coastal waters, is well documented (Ewing 1950; LaFond 1962; Perry & Schimke 1965). The bands are caused by periodic changes in the character of the surface-wave field, changes which propagate with the internal waves and locally alter the average reflexion by the sea surface. Slicks are characterized by decreased mean-square slope of the sea surface and hence a decrease in the average angle of reflexion (measured

† Present address: Marine Sciences Branch, Department of the Environment, c/o Defence Research Establishment Pacific, F.M.O., Victoria, B.C.

from the horizontal) of incident light. Seen from the air, slicks may appear either dark or light relative to the surroundings, depending upon the angle of viewing. An aerial photograph (figure 1, plate 1) of the Strait of Georgia, between Vancouver Island and the British Columbia mainland coast, shows the distinctive banded patterns associated with groups of internal waves which occur in this region. The slicks (narrow bands) here appear light toward the top and darker toward the bottom of the photograph.

The generally accepted explanation of the changes of surface reflexion in the presence of internal waves has been that of Ewing (1950), who states that slicks are caused "by the ripple-damping action of a surface film of organic matter which occurs naturally on biologically productive waters". The presence of a surface film lowers the surface tension from that of pure water by an amount which depends upon the film area; over-extended films break up into patches and have little effect on surface tension, while a film under sufficient compression will become practically inextensible. Between these extremes the film is essentially elastic; that is, the surface tension varies linearly with surface area. Lamb (1897) finds a purely viscous damping time (time for the wave amplitude to decrease to e^{-1} of its original value) of $\tau \simeq 0{\cdot}7\lambda^2$ s for a wave of length λ cm on a clean water surface, while damping times in the presence of an inextensible surface film decrease to $\tau' \simeq 0{\cdot}32\lambda^{1{\cdot}75}$ s for capillary waves and $\tau'' \simeq 0{\cdot}38\lambda^{1{\cdot}25}$ s for gravity waves (Phillips 1966). Thus the presence of a surface film greatly increases the damping of surface waves.

If an organic film covers the water surface of an area traversed by internal waves the periodic convergence and divergence of the horizontal surface current due to the internal waves will cause a periodic contraction and expansion of the surface film, with maximum extension of the film over the internal wave crests and maximum compression over the troughs. Thus, an internal wave trough would be marked by a slick, characterized by reduced ripple action due to the compacted film, and a crest would be marked by an increased number of ripples, presumably quickly regenerated by the wind.

The surface of the Strait of Georgia is 'dirty', as is indicated by the logs, wood chips, foam, etc., frequently observed in areas of convergence, so large areas may well be covered by the thin organic film necessary for the above mechanism of slick formation. However, in this region the rough bands, seen from a low altitude in figure 2 (plate 2), are characterized by sharply peaked short gravity waves which have very long crests aligned approximately parallel to the axis of the rough band; that is, parallel to the crest of the internal wave. The surface-film mechanism affects only the amplitudes, not the directions, of the various components of the surface-wave field, and its failure to account for the peculiar nature of the observed wave field in the rough bands led us to investigate an alternative mechanism – the interaction between surface waves and a periodic 'mean current' induced by the internal waves. In § 2 the effect of this current on part of the surface-wave field is examined, using simple wave kinematics and the energy equation, while in § 3 we examine the nature of a singularity of the system which gives rise to propagation barriers and adjacent prohibited areas for various components of the surface-wave field.

2. Radiation stress effects on the surface-wave field

We consider an internal-wave field propagating in the y direction only and at one speed only. Its wavelength is taken to be long enough for it to exhibit no appreciable variation in horizontal velocity over the depth containing substantially all of the motion of the surface-wave field. Its accelerations are also taken small enough for vertical displacements of the free surface due to the internal wave to be negligible (Thorpe 1968). We also consider a simple monochromatic surface wave of amplitude a, wavenumber $\mathbf{k}$ and frequency ω. The basic co-ordinate system shown in figure 3 (a) is taken with y axis in the direction of $\mathbf{c}_i$, the

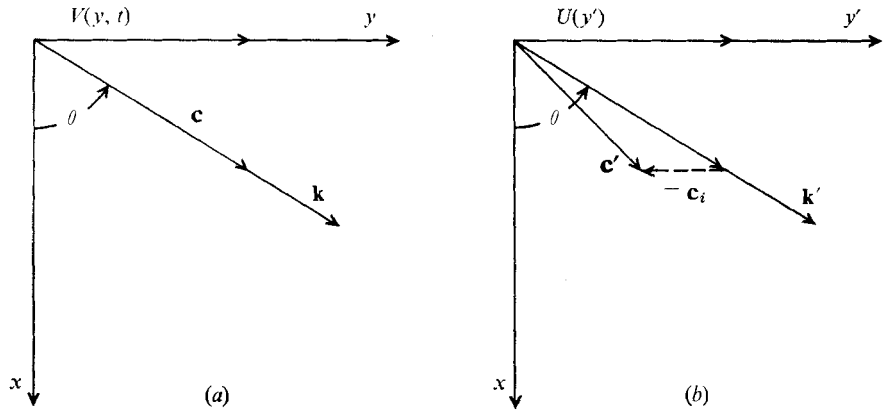

FIGURE 3. Co-ordinate systems used in the discussion of interaction between the mean current and background surface-wave field. (a) System fixed relative to source of waves, (b) system moving at uniform velocity $\mathbf{c}_i$.

direction of internal-wave propagation, so that the surface-wave vector $\mathbf{k}$ makes an angle θ with the x axis, and the phase velocity $\mathbf{c}$ is parallel to $\mathbf{k}$ in the absence of a mean current. The internal wave-induced 'mean' current $U(y-c_i t)$ will affect both the amplitude and wavenumber of the surface wave. A convenient co-ordinate system will be one moving in the positive y direction at speed c_i (figure 3 (b)) in which the motion can be considered steady (except of course for the periodic nature of the surface-wave motion). Primes will denote variables in this system, where $\mathbf{c}' = \mathbf{c} - \mathbf{c}_i$ and the mean current $U(y')$ is now time-independent. The problem is now similar to that solved by Longuet-Higgins & Stewart (1964) and in fact the analysis that follows is based on their methods (see also Phillips 1966, § 3.7). When observed in this steady-state system the surface-wave frequency ω' must be constant (Phillips 1966, § 3.5), and since lengths are invariant with respect to translation $\mathbf{k}' = \mathbf{k}$, i.e.

$$\omega' = \mathbf{k}'.(\mathbf{c}'+\mathbf{u}) = \mathbf{k}.(\mathbf{c}-\mathbf{c}_i+\mathbf{u}) = \text{constant}.$$

To this are added the dispersion relation for gravity waves on deep water, $\omega^2 = gk$, and the condition that $k_x = k\cos\theta$, the x component of the wavenumber vector, be constant. Since the mean current varies only with y' there is no mechanism for changing k_x. If, then, c_0, k_0 and θ_0 are the wave speed and the magnitude and

orientation of the wavenumber vector when $U(y') = 0$, these conditions form a set of three algebraic equations:

$$k(c + (U - c_i)\sin\theta) = k_0(c_0 - c_i \sin\theta_0), \tag{1}$$

$$c^2 k = c_0^2 k_0, \tag{2}$$

$$k\cos\theta = k_0 \cos\theta_0, \tag{3}$$

from which c, k and θ can be determined as functions of y' once $U(y')$ is specified. Before carrying out this solution, however, we examine the balance of surface wave energy; the requirement that the energy be positive and finite will result in restriction of the range of variables for which the purely kinematic relations (1)–(3) are valid.

The general equation obeyed by the wave energy as derived by Longuet-Higgins & Stewart (1964) is

$$\frac{\partial E}{\partial t} + \frac{\partial}{\partial x_j}(E(V_j + c_{gj})) + S_{ij}\Gamma_{ij} = 0,$$

where $\mathbf{V}$ is the mean velocity, $\mathbf{c}_g$ the group velocity, $S = (S_{ij})$ the radiation stress tensor of the surface wave and $\Gamma = (\Gamma_{ij}) = (\partial V_i/\partial x_j)$ the rate of strain tensor of the (horizontal) mean velocity. Observed in the x, y' system, the local time rate of change is zero. For surface waves in deep water $\mathbf{c}_g = \frac{1}{2}\mathbf{c}$ so that $\mathbf{c}_g' = \frac{1}{2}\mathbf{c} - \mathbf{c}_i$, while the radiation stress tensor is given by

$$S = \tfrac{1}{2}E \begin{pmatrix} \cos^2\theta & \sin\theta\cos\theta \\ \sin\theta\cos\theta & \sin^2\theta \end{pmatrix}$$

if the wave travels at an angle θ to the x axis. In the case of flow associated with internal waves the continuity balance of the mean flow is maintained by a vertical velocity. Thus the rate of strain tensor is simply

$$\Gamma = \begin{pmatrix} 0 & 0 \\ 0 & \partial U/\partial y' \end{pmatrix},$$

since the y' axis was chosen in the direction of the mean current, assumed to be independent of x. The energy equation thus reduces to

$$\frac{\partial}{\partial y'}[E(U - c_i + \tfrac{1}{2}c\sin\theta)] + \tfrac{1}{2}E\sin^2\theta\frac{\partial U}{\partial y'} = 0,$$

which can be integrated exactly if use is made of (1) and (3), differentiated with respect to y'. The result is

$$\frac{E}{E_0} = \frac{c_{g0}\sin\theta_0 - c_i}{c_g\sin\theta - c_i + U}\frac{\omega}{\omega_0},$$

where E_0 is a reference energy occurring when $U = 0$, that is, over a node of the interface displacement. The wave energy E is obviously positive and finite only if $c_g\sin\theta - c_i + U$ has the same sign everywhere, the simple physical requirement that the magnitude of the mean current $|U(y')|$ be less than $|c_g\sin\theta - c_i|$, the magnitude of the velocity of wave-energy propagation in the y' direction. Surface waves having velocity $\mathbf{c}_g$ such that this condition is more than marginally

satisfied will be termed the background wave field. Those waves for which $c_g \sin\theta - c_i + U = 0$ for some value within the range of U are unable to propagate through this critical position; the distribution of the critical positions is outlined in § 3. We now consider in greater detail the effect of U on the background wave field.

The wavenumber changes can be derived from the kinematic relations (1)–(3). Eliminating c and k, we obtain an equation for $\cos\theta$:

$$\frac{\cos\theta}{\cos\theta_0} - a_0\left(\frac{\cos\theta}{\cos\theta_0}\right)^{\frac{1}{2}} = \operatorname{sgn}(\sin\theta_0)\frac{a_0(U-c_i)}{c_0}(1-\cos^2\theta)^{\frac{1}{2}},$$

where $a_0 = c_0/(c_0 - c_i\sin\theta_0)$ and $|a_0| > 1$ for waves of the background field travelling in the same direction as the internal wave (the 'same' direction being defined as **c** within $\pm 90°$ of $\mathbf{c}_i$, so that $\sin\theta_0 > 0$). This equation may be treated as a

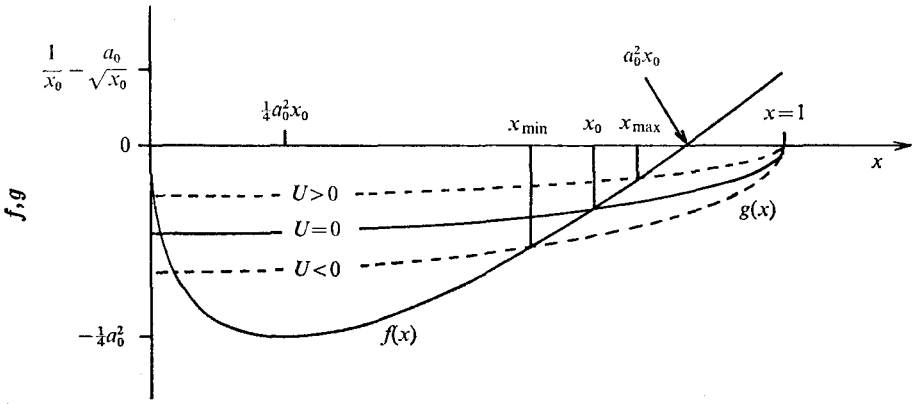

FIGURE 4. Graphical solution of the transcendental equation

$$f(x) = (x/x_0) - a_0(x/x_0)^{\frac{1}{2}} = R(y')(1-x^2)^{\frac{1}{2}} = g(x).$$

transcendental equation for $\cos\theta$, the solution varying with the value of $U(y')$. For ease in plotting, the equation is rewritten in the form

$$f(x) \equiv x/x_0 - a_0(x/x_0)^{\frac{1}{2}} = R(y')\,(1-x^2)^{\frac{1}{2}} \equiv g(x), \tag{4}$$

where $$x = \cos\theta, \quad x_0 = \cos\theta_0$$

and $$R(y') = \operatorname{sgn}(\sin\theta_0)\frac{a_0(U(y')-c_i)}{c_0}.$$

Figure 4 illustrates the two functions f and g in the interval $[0, 1]$ with $R < 0$. If $R > 0$ the set of three curves representing $g(x)$ possesses the same elliptical form but appears above the x axis.

The general behaviour of the solution of (4) is as follows.

(i) If $1 < a_0 < 2/(1+x_0^2)$, i.e. if $c_{g0} > (c_i/\sin\theta_0)$, $\cos\theta > \cos\theta_0\,(\theta < \theta_0)$ for $U > 0$ and $\cos\theta < \cos\theta_0\,(\theta > \theta_0)$ for $U < 0$, with a slight asymmetry about $x = x_0$.

(ii) If $a_0 < 0$ or $a_0 > 2/(1+x_0^2)$, i.e. if $c_{g0} < (c_i/\sin\theta_0)$, $\cos\theta < \cos\theta_0(\theta > \theta_0)$ for $U > 0$ and $\cos\theta > \cos\theta_0(\theta < \theta_0)$ for $U < 0$.

Condition (i) describes wave groups that 'overtake' the internal wave along the direction of $\mathbf{c}_i$; for condition (ii) the wave groups are 'overtaken'. From (3),

(i) results in $k < k_0$ for $U > 0$ and $k > k_0$ for $U < 0$. Thus background field waves incident in the first quadrant experience an increase in wavenumber magnitude and a turning of the wavenumber vector towards the y' axis over the crest of the internal wave ($U < 0$), and a decrease in wavenumber magnitude and a turning of the wavenumber vector away from the y' axis over the internal wave trough ($U > 0$). Examination of the solution to (4) for $-1 \leqslant \cos\theta_0 \leqslant 0$ shows that exactly the same statement can be made for θ_0 in the second quadrant, so that the directional spectrum of the background field is narrowed towards the direction of $\mathbf{c}_i$ over internal wave crests and broadened over troughs. For condition (ii) the opposite behaviour occurs, with the result that the directional spectrum is broadened over crests and narrowed over troughs. If θ_0 is in the third or fourth quadrants, $0 < a_0 < 1$ and variations in the wave spectrum are similar to those for condition (ii). These wave groups can also be considered as of the 'overtaken' variety.

The associated amplitude changes can be obtained directly from the expression for the energy, since $E \propto a^2$ for waves on a horizontal mean surface. It can be shown that for the background field the amplitude varies in the same manner as $(\omega/\omega_0)^{\frac{1}{2}}$, so that for waves satisfying condition (i) the amplitudes increase over the crests of the internal wave and decrease over the troughs. For condition (ii) the amplitudes decrease over the crests and increase over troughs.

Thus, provided that most of the background wave field travels in the same direction ($\pm 90°$) as the internal wave, this mechanism for waves satisfying condition (i) results in rough bands (increased amplitudes, decreased wavelengths, wave crests tending to be parallel to the internal crests) over the crests of an internal wave with maximum effect over the peak, while troughs are marked by relatively smooth bands (decreased amplitudes, increased wavelengths, wave crests tending to turn perpendicular to the internal troughs) and vice versa for condition (ii). The change in mean-square slope arises through changes in both the amplitude and wavelength of the surface waves, as opposed to the surface-film mechanism, which can produce only amplitude changes. As well, the wave–current interaction mechanism produces directional changes in the background wave field and is conservative in nature, unlike the mechanism of wave damping by a surface film which must rely on the wind to rebuild the wave field between slicks. Of course if most of the background wave field travels in the opposite direction to the internal wave, slicks will be produced over the crests and rough bands over the troughs of the internal wave. In this connexion it is interesting to note that most situations in which observations have been made of the relative position of slicks and internal displacements probably satisfy the condition that the surface-wave field has the same direction as the internal waves. Ewing, for example, reports internal waves in the area of San Diego that travel in a general shoreward direction (see also Lee 1961); near an open coast the surface-wave field may be expected to be within $\pm 90°$ of the on-shore direction. The internal waves in the Strait of Georgia travel roughly south to north, the prevailing wind in this area being from the south-east, so that the wind-generated surface waves will generally be travelling in the same direction ($\pm 90°$) as the internal waves. Measurements by LaFond (1962) indicate that

in his situation slicks were usually observed over the descending part of the internal wave somewhere between the wave crest and trough. In contrast, the background field analysis predicts slicks or rough patches directly over the crest or trough. (These are in fact symmetrically placed over the peaks if the current is symmetrical since the modification to the surface waves depends only on U.)† Thus the background wave field alone is not sufficient to explain some features of the observed banded patterns.

Another striking feature not explained by the background field is the sharply-peaked, long-crested waves which are observed travelling with crests roughly parallel to the axis of the rough bands. The highly nonlinear character of the surface wave field in the rough bands is consistent with the view that the dominant interaction is a preferential growth of surface waves for which the energy propagation velocity somewhere equals the phase speed of the internal wave. These are the waves that give rise to critical positions.

3. Singularities in E

In figure 4 there is the possibility that the crossings of the f and g curves can merge (as for a_0^2 near 4) and so provide real roots for some values of U and not for others. It is the purpose of this section to identify the coalesced roots as giving rise to singularities in the energy density and to provide illustrations of the surface-wave field for some cases of coalescence. Let us examine the wavenumber equation (4) written in rectangular co-ordinates:

$$k_y(U-c_i)+g^{\frac{1}{2}}(k_y^2+k_x^2)^{\frac{1}{4}} = -k_{y0}c_i+g^{\frac{1}{2}}(k_{y0}^2+k_x^2)^{\frac{1}{4}}. \tag{5}$$

This can be rewritten as $F(k_y, k_{y0}, k_x, U, c_i) = 0$. It should be noted that F depends only on k_x^2 so any results obtained for $+k_x$ are equally valid for $-k_x$. The solution for the energy ratio can be written as

$$\frac{E}{E_0} = \left(\frac{k_x^2+k_y^2}{k_x^2+k_{y0}^2}\right)^{\frac{1}{4}} \frac{\partial F/\partial k_{y0}}{\partial F/\partial k_y}. \tag{6}$$

From (5) it is seen that k_y becomes infinite only if k_{y0} does, and in this limit $k_y/k_{y0} \to c_i/(c_i-U)$. Therefore singularities in E occur only for those wavenumbers such that $F = 0$ and $\partial F/\partial k_y = 0$ simultaneously, i.e. at repeated roots of F. Let us non-dimensionalize the variables in (5) by dividing through by $(g|k_x|)^{\frac{1}{2}}$. With $k_y/|k_x| = \eta$, $P = (c_i-U)/(g/|k_x|)^{\frac{1}{2}}$, ($P > 0$ everywhere) and

$$Q = (g|k_x|)^{\frac{1}{2}}/(\text{right-hand side of (5)}) = (g|k_x|)^{\frac{1}{2}}/\omega_0',$$

$$(\eta^2+1)^{\frac{1}{4}} = P\eta + 1/Q \tag{7}$$

or

$$F(\eta, P, Q) = 0.$$

The form of F thus guarantees that (5) has either three real roots or one real root and two complex conjugates. Each of these three roots describes waves which have (in general) quite distinct wavelengths and directions of propagation at $U = 0$, including directions opposite to $\mathbf{c}_i$. The only limitation is that they all have the same value of P and the same value of Q. A repeated root can thus be

† This symmetry is also a feature of the waves which experience critical positions.

thought of as a coalescence of more than one wave into a single wavenumber at the position of the root. If the singularity is due to a double root there are wave trains which have real but different wavenumbers on one side of the critical position and which coalesce and have complex wavenumbers on the other and thus are exponentially eliminated. If the singularity is due to a triple root (possible if $P = (108)^{-\frac{1}{4}}$, $Q = (27/16)^{\frac{1}{2}}$ somewhere) one real wave train and two complex ones exist on each side of the critical position. At the triple root position $\eta = \sqrt{2}$. In figure 4 two intersections of f and g have been explicitly shown and only one of these has been examined in any detail. Apart from a simple scale change in the ordinate for both f and g, an identical set of curves can be obtained in which x_0 pertains to the other crossing, thus making it a legitimate root. It is only necessary that both sets of curves have the same value of $a_0^2 x_0$ (which in fact equals Q). A similar situation exists for the third root (which may be on the same side of the x axis as the other two, e.g. $a_0^2 x_0$ slightly larger than 1).

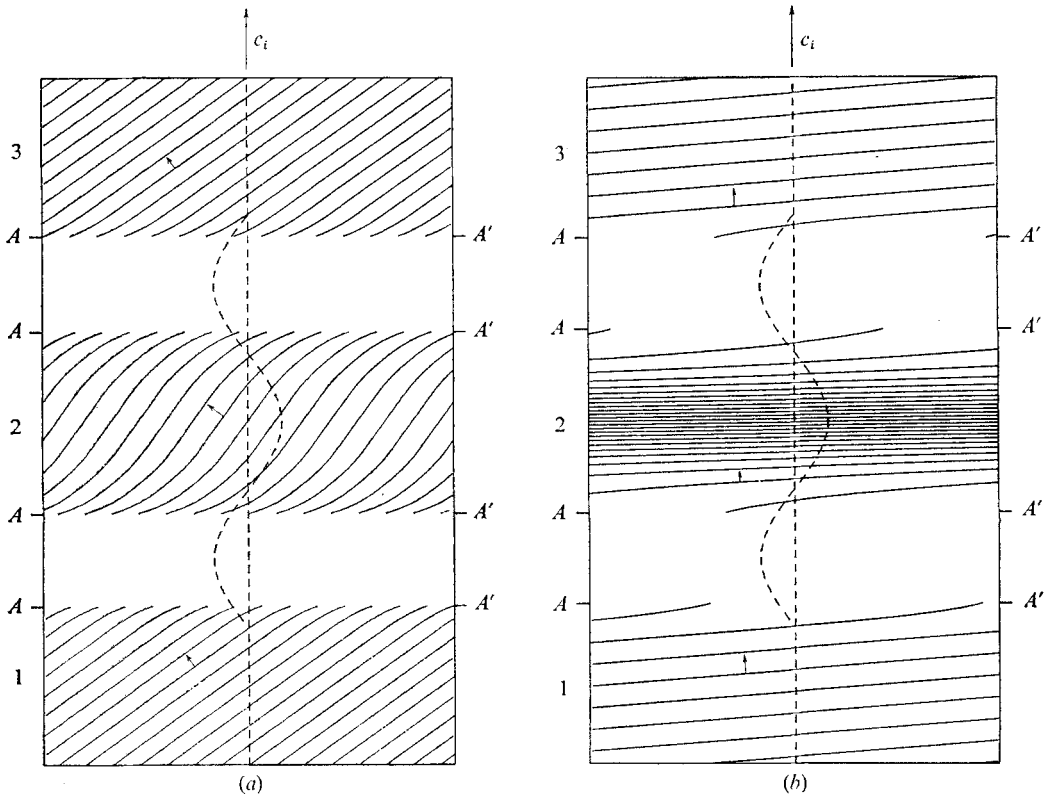

FIGURE 5. Plan view of the shapes of surface-wave crests. The broken lines down the centre of the illustration represent $U(y')$, which is positive to the right. For simplicity, the internal wave is sinusoidal and 1·5 periods long only. It is propagating towards the top of the page at a phase velocity of 0·626 m/s and has a wavelength of 100 m. Thus $U > 0$, a positive current, means fluid flowing towards the top of the page. The positions AA' indicate double-root critical positions and the small arrows indicate the direction of surface-wave energy propagation. The surface-wave parameters are $k_x = -1{\cdot}0$ m^{-1} and (*a*) $k_{y0} = 1{\cdot}412$ m^{-1}, every tenth surface wave shown; (*b*) $k_{y0} = 12{\cdot}63$ m^{-1}, every hundredth wave shown.

It should be mentioned that this analysis breaks down at the singularities and thus no answers can be given to the interesting and important questions regarding reflexion versus absorption of energy, or of continuation of the wave field across critical positions.

Figures 5 (*a*) and (*b*) show the plan view shape of surface wave crests for a particular numerical case. This case was chosen to illustrate the coalescence of two waves at critical positions (represented by the positions AA') and the elimination of the surface-wave field from regions over the internal wave between these positions. The small arrows indicate the direction of the surface-wave energy propagation. The broken lines in the centre of the figures represent $U(y')$, which is sinusoidal for 1·5 periods and zero elsewhere (at the top and bottom of the figure). The internal wave values for c_i and wavelength were chosen as 0·626 m/s and 100 m respectively and the surface-wave nodal values are as follows: $k_x = -1{\cdot}0\,\mathrm{m}^{-1}$, $k_{y0} = 1{\cdot}412\,\mathrm{m}^{-1}$ in figure 5 (*a*) (with every tenth wave shown) and $k_{y0} = 12{\cdot}63\ \mathrm{m}^{-1}$ in figure 5 (*b*) (with every hundredth wave shown). The peak value of $|U|/c_i$ is 0·5. The critical positions are the same in both figures and occur at $U/U_{\mathrm{peak}} = -0{\cdot}5$.

In these examples the initial conditions would determine whether the surface-wave field contained any energy in regions 2 and 3. If either of these examples is considered to be one Fourier component of a real wind–wave system, the initial conditions would still be important; however, there would be local wave generation in regions 2 and 3 which would be Doppler shifted because of U. An examination of the surface-wave field under those conditions is beyond the scope of this analysis.

Figure 6 presents the case of a triple root for the same internal wave conditions as in figure 5, except that $c_i = 1{\cdot}5$ m/s, and for $k_x = -1{\cdot}0\,\mathrm{m}^{-1}$ and $k_{y0} = 0{\cdot}301\,m^{-1}$. Again every tenth wave is shown. The triple-root critical positions† are at AA', where $U/U_{\mathrm{peak}} = 0{\cdot}707$. There are no forbidden regions in this case (in contrast with figure 5) because even though the first and second derivatives of k_y are infinite at AA', k_y itself is continuous and possesses one real value everywhere. We have emphasized the existence of a triple root for two reasons. First, we expect that a solution to the problem using asymptotic expansions which are uniformly valid across all critical positions will be governed by the nature of the expansion near the triple root. We are at present investigating this problem. Second, but not independently, the triple root represents the highest order singularity in wavenumber space and should thus produce the most profound effect on the surface waves. Whether this is readily apparent will depend on the relative amount of surface-wave energy in wavenumbers that give rise to a triple root compared with that of those that do not, and of the effect of $(\omega/\omega_0)^{\frac{1}{2}}$.

Finally, figure 7 presents the nodal parameters that give rise to critical positions somewhere in an internal wave field as a function of the internal-wave magnitude. The parameter that determines the various curves in figure 7 (*a*) is $q = U_{\mathrm{min}}/c_i$ and in figure 7 (*b*) it is $q = U_{\mathrm{max}}/c_i$. The numbers that are displayed are the q values for the representative curves. The curves labelled Γ are the envelopes

† We have shown the wave crests continuous across the critical positions here, thus anticipating that a uniformly valid and everywhere finite asymptotic expansion does exist.

of the end points of individual q curves. The co-ordinates in figure 7 are most conveniently represented in polar form: the radius vector has a magnitude of $\omega_0 c_i/g$ (where ω_0 is the nodal radian frequency of the surface waves) and a direction θ_0 (the nodal propagation direction of the surface). The internal wave is propagating along $\theta_0 = 90°$. The area contained between curves which have the

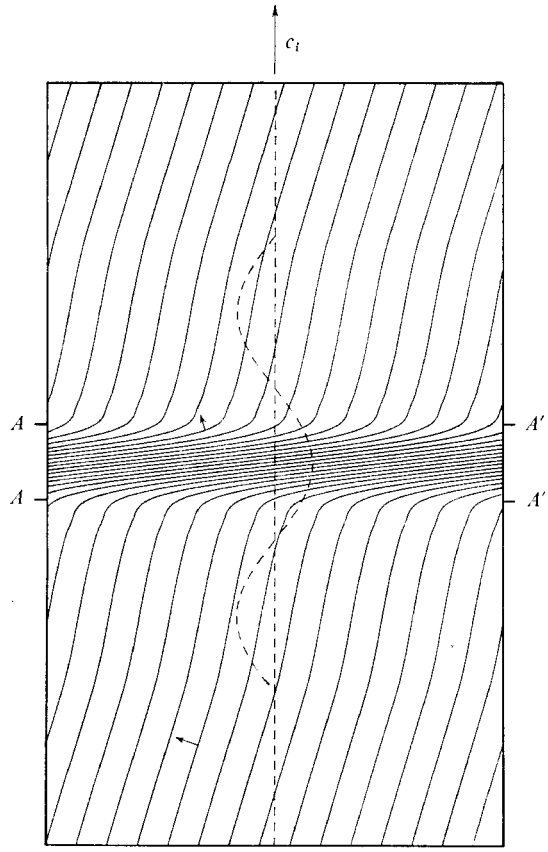

FIGURE 6. As in figure 5, except that $c_i = 1{\cdot}5$ m/s. $k_{y0} = 0{\cdot}301$ m^{-1} and every tenth wave is shown. The locations AA' indicate triple-root critical positions.

same q values, and which is bounded by Γ represents the nodal values of those surface waves which are eliminated somewhere in that particular internal wave field. Thus, if an internal-wave field gradually builds up from zero height in the presence of a surface wave field† and if the peak of the surface-wave energy falls in the 'eliminated' area, then a substantial change in the visual character of the surface-wave field should result merely from the existence of the singularities. The appearance would be that of a series of slicks.‡ For comparison a directional surface-wave spectral measurement of Gilchrist (1966) is also shown. The shaded

† For example, dead-water waves behind a vessel slowly changing speed.

‡ Even if the singularities represent regions of increased dissipation, permanent slicks could be formed either by establishing a balance with some regenerative process such as the local wind or by dissipating all the energy in waves encountering singularities and thus leaving apparent the band structure of the background wave field.

area represents values of the energy spectrum greater than or equal to 10% of the peak value for a fetch limited wind–wave spectrum.† The magnitude of the wind was 5·8 m/s at a height of 2 m and we have arbitrarily assigned the energy spectrum to be approximately symmetrical about $\theta_0 = 90°$ (a 45° shift, see previous

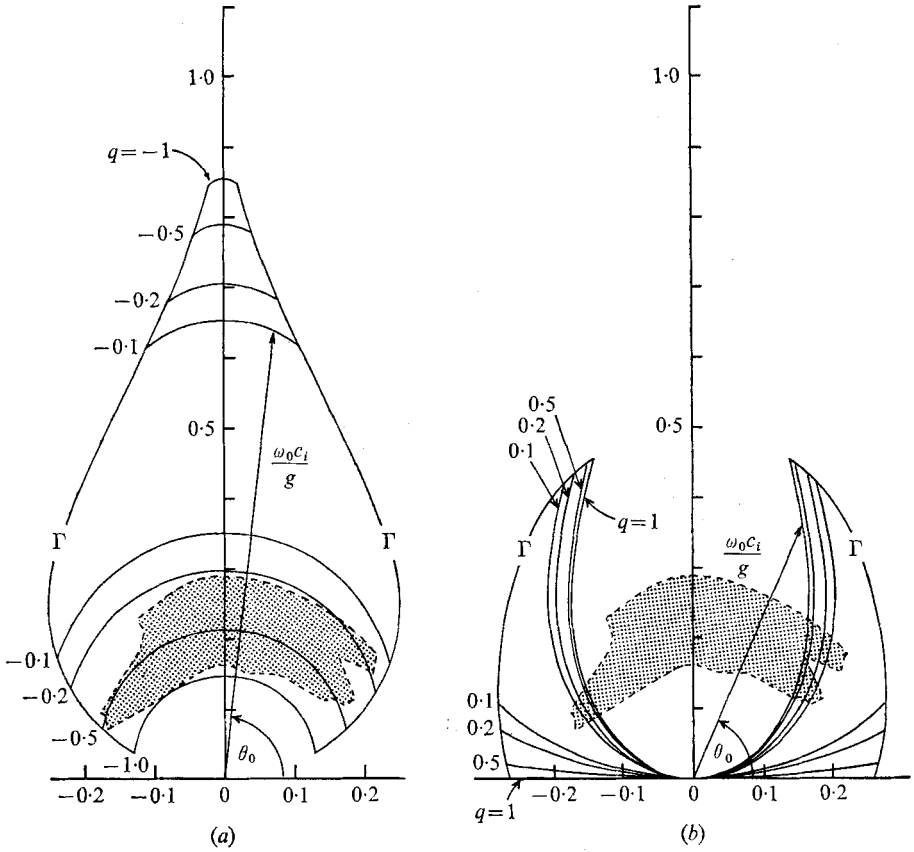

FIGURE 7. Frequency and propagation direction of those surface waves which have an important critical position somewhere in an internal wave field. The magnitude of the surface current due to the internal wave is given by $q = U_{\text{peak}}/c_i$. In polar co-ordinates the radius vector has a length of $\omega_0 c_i/g$ and an angle equal to the propagation angle of the surface waves at the nodal positions ($U = 0$), ω_0 being the radian frequency of the surface waves also at the nodal positions. The internal wave is propagating along the direction $\theta_0 = 90°$, Γ represents the loci of the end-points of the curves for the individual q's and the shaded areas represent an experimental surface wind–wave spectrum measured by Gilchrist (1966) and for which c_i was taken as 0·60 m/s. (*a*) $q < 0$, (*b*) $q > 0$.

footnote). Although internal waves were not a feature of his experimental situation we have arbitrarily taken $c_i = 0{\cdot}60$ m/s. Since the shaded area lies entirely within Γ and the bounding curves for $q = -1$ in figure 7 (*a*), strong enough (large negative q) internal waves at this c_i would produce critical positions over the

† The values shown were taken from the published curves (Gilchrist 1966, figure 8), with some extrapolations where needed. His spectrum is asymmetric with respect to the wind direction because of local fetch limitations.

majority of the surface-wave spectrum. A larger c_i would require less strong internal waves for the same effect, and for large enough c_i the spectrum will begin to fall outside Γ. It must be emphasized that this measured spectrum was taken when wave generation was an important feature of the wind–wave system and so it can only serve as a qualitative comparison.

There are critical positions which are not included in figure 7. These are of two types: those which possess complex wavenumbers at $U = 0$ and which become real only for $|U|$ greater than the critical value, and those for which the surface-wave energy can propagate through the internal-wave field if the critical positions behave as perfect reflectors. The first situation is omitted because we are restricting ourselves to real nodal values only. The second situation is omitted because the surface-wave field can exist everywhere even though critical positions are present and there are thus no areas of elimination. This case occurs if $1 < Q < (27/16)^{\frac{1}{4}}$. There are then two double-root critical positions instead of just one in each region $0 \leqslant U \leqslant U_{\max}$ and by reflecting off both barriers (in reverse order and changing wavenumber 'branches' each time) it is possible for the energy to travel through the entire field. In fact the triple root can be considered a coalescence of such a double-root pair.

A complete description of the phenomenon (e.g. as shown in figure 2) must await a non-singular theory. It can be seen, however, that the main features of this particular photograph are (i) extra large wave amplitudes in narrow spatial bands and (ii) a considerable variation in wavelength of the surface waves at different positions in the band (and propagation at a considerably different angle from a major part of the background wave field). Our suggestion is that it is possible that the wavelength separation is due to the variation of particle velocity of the internal wave and that each is at its critical position. The excess amplitude would then follow immediately. It is also possible, of course, that other simultaneous effects exist such as non-singular interactions as described in § 2 acting on a suitably non-flat surface-wave spectrum, or local generation by wind which is modified by the presence of the internal-wave particle velocity. We do suggest, however, in this case at least (and in many others of our observations) that a surface film is not a primary disturbing agency.

One of us (A. E. G.) would like to record her special thanks to Dr P. H. LeBlond of I.O.U.B.C., who acted as her supervisor during her studies there. The work presented here is based on part of her Ph.D. thesis. The other (B. A. H.) would like to express his appreciation to all the members of D.R.E.P. who contributed towards his understanding of this problem, in particular Dr H. L. Grant.

REFERENCES

EWING, G. 1950 *J. Marine Res.* **9**, 161.
GILCHRIST, A. W. R. 1966 *J. Fluid Mech.* **25**, 795.
LAFOND, E. C. 1962 In *The Sea*, vol. 1. Interscience.
LAMB, H. 1897 *Hydrodynamics*. Dover.
LEE, O. S. 1961 *Limnology & Oceanography*, **6**, 312.
LONGUET-HIGGINS, M. S. & STEWART, R. W. 1964 *Deep-Sea Res.* **11**, 529.
PERRY, R. B. & SCHIMKE, G. R. 1965 *J. Geophys. Res.* **70** (10), 2319.
PHILLIPS, O. M. 1966 *The Dynamics of the Upper Ocean*. Cambridge University Press.
SHAND, J. A. 1953 *Trans. Am. Geophys. Union*, **34** (6), 849.
THORPE, S. A. 1968 *Phil. Trans. Roy. Soc.* A **263**, 563.

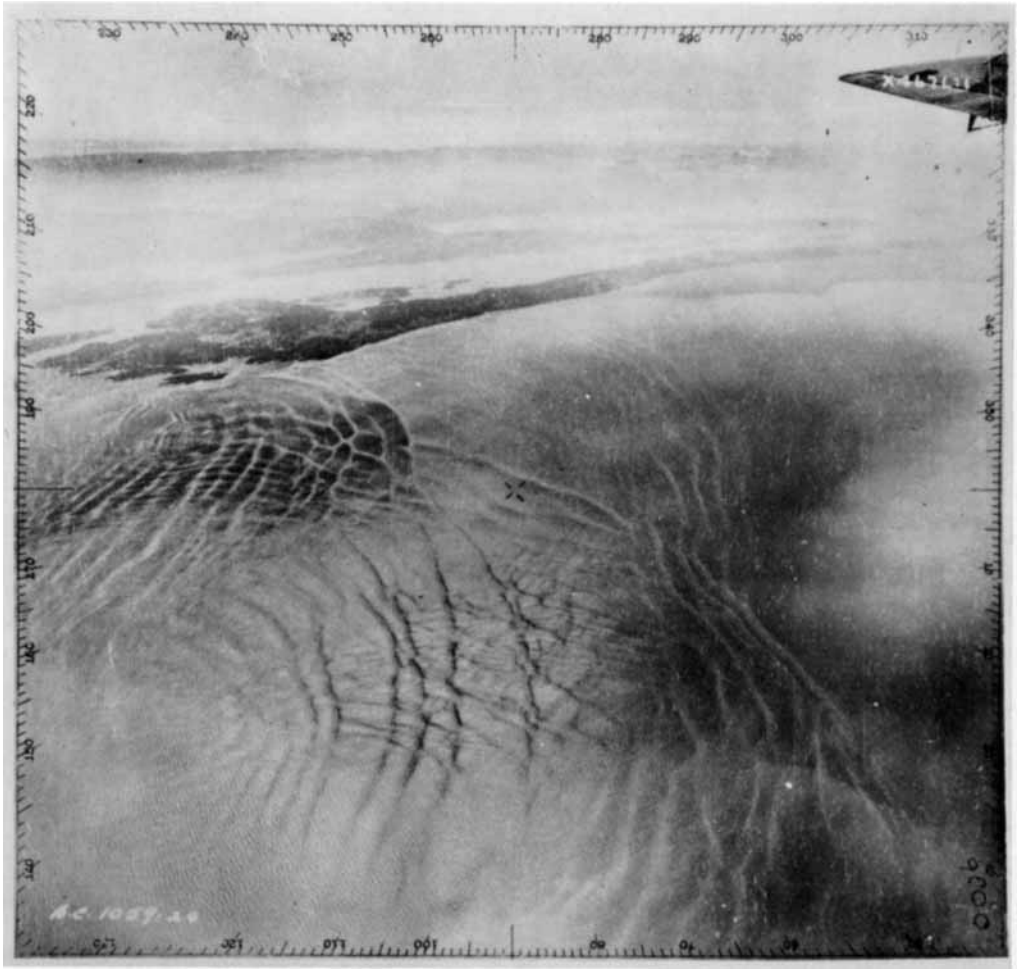

FIGURE 1. Aerial photograph showing banded surface markings produced by internal waves: Strait of Georgia, British Columbia. (Taken by the British Columbia Government in 1950 and originally published by Shand (1953).)

FIGURE 2. The banded markings as seen from a low altitude, note the sharply peaked long-crested waves parallel to the axis of the rough band. The length of the surface waves in the rough band near the bottom left corner is of order 30 cm.